Using Eurocodes and Aashto for assessing shear in slab bridges

Lantsoght, Eva; van der Veen, Cor; de Boer, A; Walraven, Joost

DOI
10.1680/jbren.14.00022

Publication date
2016

Document Version
Final published version

Published in
Proceedings of the ICE - Bridge Engineering

Bridge Engineering

Using Eurocodes and Aashto for assessing shear in slab bridges
Lantsoght, van der Veen, de Boer and Walraven

ice | proceedings

Proceedings of the Institution of Civil Engineers

http://dx.doi.org/10.1680/jbren.14.00022
Paper 1400022
Received 02/06/2014 Accepted 16/11/2015
Keywords: codes of practice & standards/concrete structures/slabs & plates

ice
Institution of Civil Engineers
publishing

Using Eurocodes and Aashto for assessing shear in slab bridges

Eva O. L. Lantsoght BSc, MSc, PhD
Researcher, Concrete Structures, Delft University of Technology, Delft, the Netherlands (corresponding author: E.O.L.Lantsoght@tudelft.nl)

Cor van der Veen BSc, MSc, PhD
Associate professor, Concrete Structures, Delft University of Technology, Delft, the Netherlands

Ane de Boer BSc, MSc, PhD
Senior adviser, Ministry of Infrastructure and the Environment, Utrecht, the Netherlands

Joost C. Walraven BSc, MSc, PhD
Emeritus professor, Concrete Structures, Delft University of Technology, Delft, the Netherlands

Reinforced concrete short-span solid-slab bridges are used to compare Dutch and North American practices. As an assessment of existing solid-slab bridges in the Netherlands showed that the shear capacity is often governing, this paper provides a comparison between Aashto (American Association of State Highway and Transportation Officials) practice and a method based on the Eurocodes, and recommendations from experimental research for the shear capacity of slab bridges under live loads. The results from recent slab shear experiments conducted at Delft University of Technology indicate that slabs benefit from transverse force redistribution. For ten selected cases of straight solid-slab bridges, unity checks (the ratio between the design value of the applied shear force and the design beam shear resistance) are calculated according to the Eurocode-based method and the Aashto method. The results show similar design shear forces but higher shear resistances in the North American practice, which is not surprising as the associated reliability index for Aashto is lower.

Notation

A_{ps}	area of prestressing steel
A_s	area of reinforcing steel
a	shear span
a_g	maximum aggregate size
a_v	clear shear span
b	full width
b_{edge}	edge distance
b_{eff}	effective width in shear
b_{eff1}	effective width from a horizontal load spreading under 45° from the centre of the load
b_{eff2}	effective width from a horizontal load spreading under 45° from far corners of the load
b_{load}	width of the load, taken in the span direction
b_r	distance between the free edge and the centre of the load
b_v	effective width: minimum web width within the depth d_v or, for slabs, the effective width
b_w	web width of section or, for slabs, the effective width
$C_{Rd,c}$	factor from NEN-EN 1992-1-1:2005 (CEN, 2005) expression for shear
$d_{asphalt}$	thickness of wearing course
d_l	effective depth to main flexural reinforcement
d_v	effective shear depth: the internal lever arm ≥ max $(0{\cdot}9d_l, 0{\cdot}72h)$
E_p	modulus of elasticity of prestressing steel
E_s	modulus of elasticity of reinforcing steel
e	eccentricity of load
F	reaction force
f'_c	concrete compressive strength
f_{ck}	characteristic cylinder compressive strength of concrete
$f_{ck,cube}$	characteristic cube compressive strength of concrete
f_{po}	parameter taken as the modulus of elasticity of prestressing tendons multiplied by the locked-in difference in strain between prestressing tendons and surrounding concrete
f_{yk}	characteristic yield strength of reinforcement bar
k	size effect factor
l_{span}	span length
M_u	factored moment, not to be taken less than $V_u d_v$
N_u	factored axial force
s_x	the lesser of d_v or maximum distance between layers of longitudinal crack control reinforcement
s_{xe}	crack spacing factor
V_c	shear capacity according to Aashto LRFD (Aashto, 2015)
V_{Ed}	design shear force
V_p	component of effective prestressing force in direction of the applied shear
$V_{Rd,c}$	design shear capacity
V_u	factored shear force

v_c	design shear resistance according to Aashto
v_{Ed}	design shear stress according to Eurocodes
v_{min}	lower bound of shear capacity
$v_{Rd,c}$	design shear resistance according to Eurocodes
v_u	design shear stress according to Aashto
$w_{th,1}$	width of design lane according to NEN-EN 1991-2:2003 (CEN, 2003) (typically 3 m)
α_{Qi}	factor to magnify truck load
α_{qi}	factor to magnify lane load
β	reduction factor for loads close to the support
β_{MCFT}	factor indicating the ability of diagonally cracked concrete to transmit tension
β_{new}	reduction factor for concentrated loads on slabs close to the support
β_{rel}	reliability index
γ_{DL}	load factor for dead load
γ_{DC}	load factor for superimposed load
γ_{LL}	load factor for live load
Δq_{load}	increased lane load on the heavily loaded lane in load model 1
ε_x	strain at mid-depth of the cross-section
ρ_l	flexural reinforcement ratio
σ_{cp}	axial stress on the cross-section (positive in compression)
τ_{add}	shear stress due to self-weight of slab and forces on prestressing bars
$\tau_{combination}$	sum of τ_{conc} and τ_{line}
τ_{conc}	shear stress due to concentrated load over the effective width
τ_{line}	shear stress due to distributed load over the full width
$\tau_{tot,cl}$	ultimate shear stress in experiment with concentrated load only
ϕ	resistance factor

1. Introduction

A large number of existing reinforced concrete bridges in the Dutch road network consist of short-span solid-slab bridges. As these bridges often have a simple geometry, they provide an excellent case for a comparison between European and North American practices. In the Netherlands, the Ministry of Infrastructure and the Environment initiated a project to assess the shear capacity of existing bridges (60% of which were built before 1975) under increased traffic loads as prescribed by the recently implemented Eurocodes. In total, the shear capacity of 600 reinforced concrete slab bridges needs to be studied. Preliminary calculations indicated that the shear capacity can be insufficient (Walraven, 2010) even though no signs of distress are observed.

The large number of solid-slab bridges to be assessed requires a systematic approach. The goal of the first round of assessments is to determine which particular bridges require a more detailed analysis; for this, a fast, simple and conservative tool is required (e.g. the quick scan method (Lantsoght *et al.*, 2013a)). The quick scan is a spreadsheet-based method, similar to extended hand calculations (Vergoossen *et al.*, 2013). The quick scans result in 'unity check' values; that is, the ratio between the design value of the applied shear force resulting from loads on the bridge according to current codes (dead loads, superimposed loads and live loads) and the shear resistance. The critical loading case on a slab occurs with a design truck close to the free edge parallel to the driving direction (Cope, 1985), and this is the case considered in the quick scan.

2. Literature survey

Although slab bridges are calculated as beams with a large width without taking the beneficial effect of the extra dimension into account, some researchers have studied the behaviour of this bridge type and showed that the capacity is larger than the rating (Aktan *et al.*, 1992; Azizinamini *et al.*, 1994a, 1994b).

The shear failure modes that need to be verified are flexural shear and punching shear. Flexural shear failure results in an S-shaped shear crack at the side face of the slab, or, if the slab is very wide, the crack can develop in the interior of the slab (Figures 1(a)–1(c)). Punching shear failure results in the punching out of a concrete cone. If sufficient flexural reinforcement is provided, the cone will not be clearly visible, but cracking on the opposite face of the load will indicate punching failure (Figures 1(d) and 1(e)). The check for flexural shear for slab bridges can be carried out with the quick scan method, where the occurring shear stress from the loads is compared with the flexural shear capacity. Punching checks are beyond the scope of this paper, but need to be carried out on a perimeter around the loads, where the occurring shear loading is compared with the punching shear capacity.

For flexural shear in wide members, an effective width needs to be determined. The effective slab width in shear is theoretically determined so that the reaction resulting from the total shear stress over the width of the support equals the reaction from the maximum shear stress over the effective width. For design purposes, a method of horizontal load spreading (depending on local practice) is chosen, resulting in the effective width b_{eff} at the support. In Dutch practice, horizontal load spreading is assumed under a 45° angle from the centre of the load towards the support (Figure 2(a)) and, in French practice, (Chauvel *et al.* 2007) from the far corners of the loading plate (Figure 2(b)). Currently, the only code that prescribes an effective width for shear in wide members is Model Code 2010 (fib, 2012) (Figure 2(c)). The UK currently has no codified practice for determining the effective width in shear.

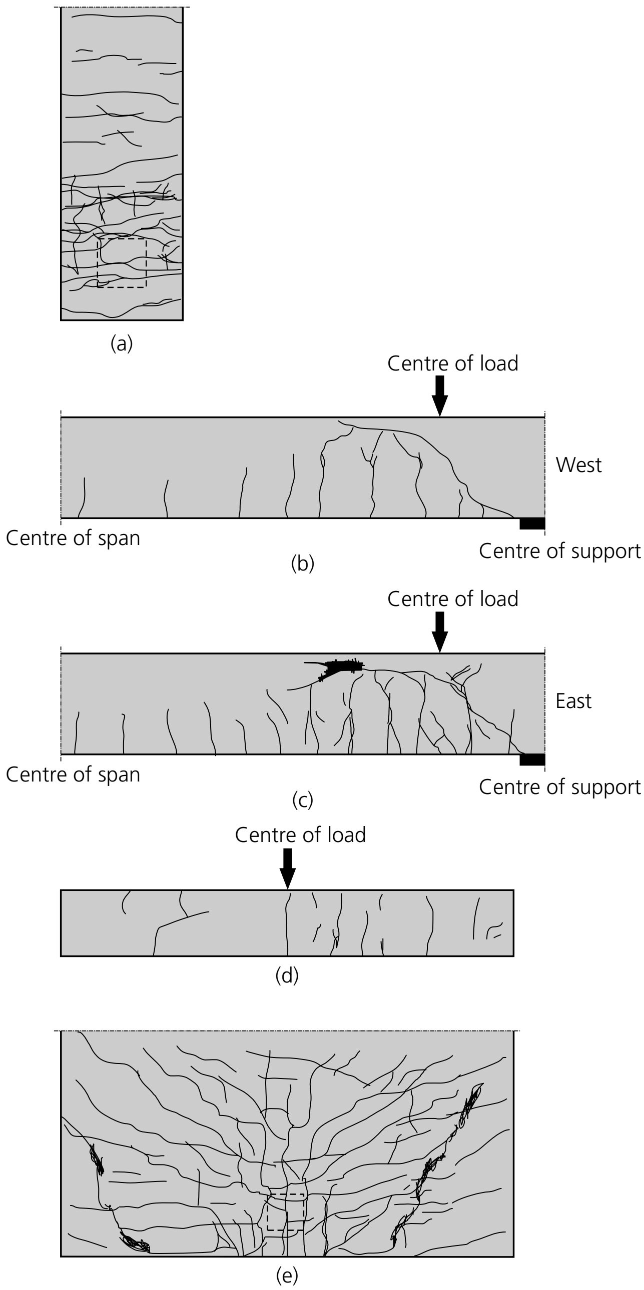

Figure 1. One-way shear: cracks after failure of BS2T1 (Lantsoght *et al.*, 2014): (a) bottom face; (b) west side face; (c) east side face. Two-way shear: cracks after failure of S9T1 (Lantsoght *et al.*, 2013c): (d) front face; (e) bottom face

3. Comparison of Eurocodes and North American code provisions

3.1 Live load

In load model 1 of NEN-EN 1991-2:2003 (CEN, 2003) (Figure 3), a tandem system (design truck) is combined with a uniformly distributed load (design lane load). The tandem system has a tyre contact area of 400 mm × 400 mm and an axle load of $\alpha_{Q1} \times 300$ kN in the first lane, $\alpha_{Q2} \times 200$ kN in the second lane and $\alpha_{Q3} \times 100$ kN in the third lane. The α_{Qi} are nationally determined parameters that can be used to tailor the Eurocode load model to the traffic loading situation of individual countries. All α_{Qi} equal the recommended value of 1. The uniformly distributed load is applied over the full width of the lane and is $\alpha_{qi} \times 9$ kN/m^2 for the first lane and $\alpha_{q1} \times 2{\cdot}5$ kN/m^2 for all other lanes, with α_{qi} being nationally determined parameters. In the Netherlands, for bridges with three or more notional lanes, $\alpha_{q1} = 1{\cdot}15$ and, for $i > 1$, $\alpha_{qi} = 1{\cdot}4$.

In Aashto LRFD (American Association of State Highway and Transportation Officials load and resistance factor design) (Aashto, 2015), a combination of a design truck or design tandem with a design lane load is considered (Figure 4). The tyre contact area is 510 mm × 250 mm for design truck and tandem. The design truck has three axle loads: 35 kN and two times 145 kN. The longitudinal spacing between the two 145 kN axles is varied between 4300 mm and 9000 mm to produce extreme force effects. The transverse spacing is 1800 mm. The design tandem consists of a pair of 110 kN axles spaced 1200 mm apart and with a transverse spacing of 1800 mm. A dynamic load allowance (IM) of 33% has to be considered for both the design truck and the design tandem (Aashto, 2015: table 3.6.2.1-1). The design lane load from Aashto LRFD consists of a load of 9·3 N/mm uniformly distributed in the longitudinal direction. Transversely, the design lane is assumed to be uniformly distributed over a 3 m width, which is smaller than the full lane width (3·6 m). This width marks the largest difference in the way the Eurocode and Aashto prescribe the lane load.

3.2 Shear capacity

According to §6.2.2(1) of NEN-EN 1992-1-1:2005 (CEN, 2005), the shear resistance for a member without stirrups is calculated as

$$1.\quad V_{\mathrm{Rd,c}} = \left[C_{\mathrm{Rd,c}} k (100\rho_{\mathrm{l}} f_{\mathrm{ck}})^{1/3} + k_1 \sigma_{\mathrm{cp}}\right] \times b_{\mathrm{w}} d_{\mathrm{l}} \geq (v_{\min} + k_1 \sigma_{\mathrm{cp}}) b_{\mathrm{w}} d_{\mathrm{l}}$$

$$2.\quad k = 1 + \sqrt{\frac{200}{d_{\mathrm{l}}}} \leq 2{\cdot}0$$

where all the terms are defined in the notation list, d_{l} is in mm and $k_1 = 0{\cdot}15$. Equation 1 is an empirical relation, first

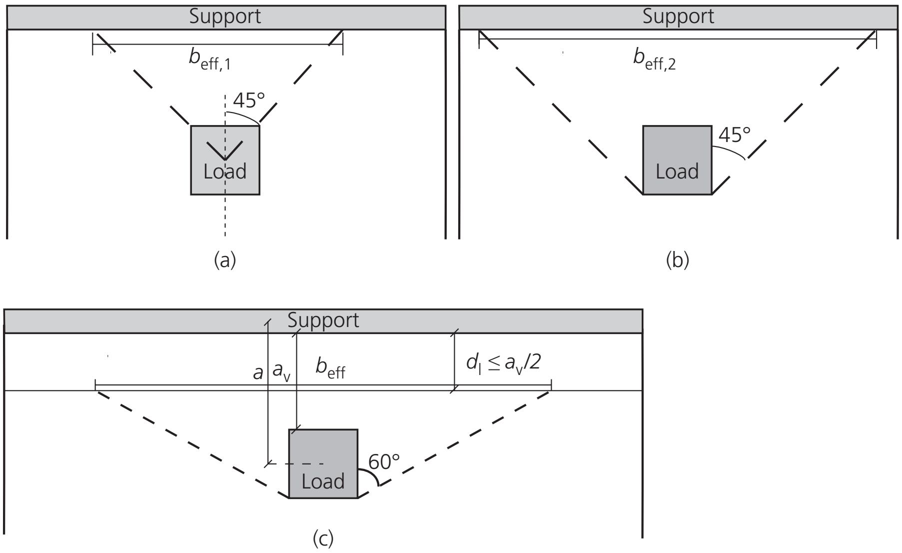

Figure 2. Effective width (a) assuming 45° horizontal load spreading from the centre of the load (b_{eff1}) and (b) assuming 45° horizontal load spreading from the far corners of the load (b_{eff2}); (c) top view of slab as prescribed by Model Code 2010 (fib, 2012)

proposed by Regan (1987) based on experimental results (Lantsoght *et al.*, 2015d, 2015e). According to the Eurocode procedures, the values of the factor $C_{Rd,c}$ and the lower bound of the shear capacity v_{min} may be chosen nationally. The default values are $C_{Rd,c} = 0{\cdot}18/\gamma_c$ with $\gamma_c = 1{\cdot}5$ and v_{min} (f_{ck} in MPa) given by

3. $$v_{min} = 0{\cdot}035k^{3/2}f_{ck}^{1/2}$$

The contribution of a load applied within a distance $0{\cdot}5d_l \leq a_v \leq 2d_l$ from the edge of a support to the shear force V_{Ed} may be multiplied by the reduction factor $\beta = a_v/2d_l$ (CEN, 2005: §6.2.2(6)) as a result of direct transfer of the load from its point of application to the support.

The Aashto load and resistance factor rating (LRFR) (Aashto, 2011: §6A.5.8) mentions that in-service concrete bridges showing no visible signs of shear distress need not be checked for shear when rating for the design load. This code requirement is not in line with the current practice in several European countries, where all existing bridges need to be rated for shear as a result of the increased live loads and new shear models. When shear rating is carried out, the critical section for shear is taken at the face of the support (Aashto, 2015: §5.13.3.6.1). The sectional design model, based on modified compression field theory (MCFT) (Vecchio and Collins, 1986),

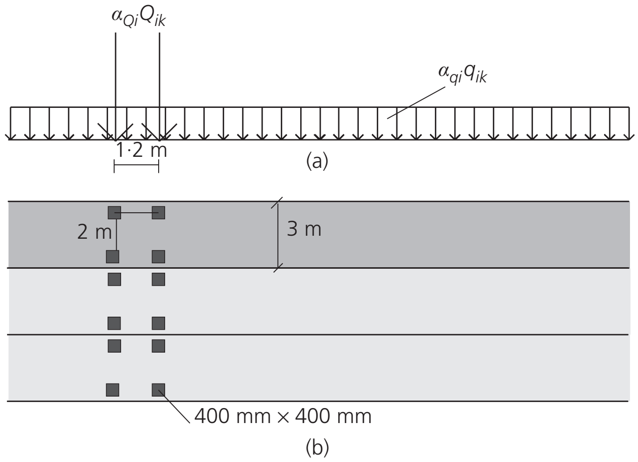

Figure 3. Traffic loads according to NEN-EN 1991-2:2003 (CEN, 2003): (a) side view; (b) top view

is given in §5.8.3. MCFT describes the stress–strain relationships for cracked concrete. In a member without transverse reinforcement, the shear capacity depends fully on the concrete contribution V_c, given by

4. $$V_c = 0{\cdot}083\beta_{MCFT}\sqrt{f'_c}b_v d_v$$

where d_v is the effective shear depth: the internal lever arm ≥ max($0{\cdot}9d_l$, $0{\cdot}72h$). The value of β_{MCFT} can be found in Aashto (2015: §5.8.3.4.2)

$$\beta_{MCFT} = \frac{4{\cdot}8}{1+750\varepsilon_s}\frac{1300}{990+s_{xe}} \quad (5)$$

depending on the crack spacing factor s_{xe} and the strain ε_x

$$300\ \text{mm} \leq s_{xe} = s_x\frac{35}{a_g+16} \leq 2000\ \text{mm} \quad (6)$$

where s_x is the lesser of either d_v or the maximum distance between layers of longitudinal crack control reinforcement, a_g is the maximum aggregate size and

$$\varepsilon_x = \frac{\left(|M_u|/d_v + 0{\cdot}5N_u + |V_u - V_p| - A_{ps}f_{po}\right)}{E_sA_s + E_pA_{ps}} \leq 6\times10^{-3} \quad (7)$$

The sectional moment has to fulfil

$$|M_u| \geq |V_u - V_p|d_v \quad (8)$$

The resistance factor for shear is $\phi = 0{\cdot}90$ (Aashto, 2015: §5.5.4.2.1).

3.3 Load factors

The Eurocode suite only provides load and resistance factors for design and the Eurocodes for rating and assessment are under preparation. To allow for assessment according to the basic assumptions and philosophy of the Eurocodes (Lantsoght *et al.*, 2015c), a set of national codes is being developed in the Netherlands: NEN 8700 for the basic rules (NEN, 2011a), NEN 8701 for actions (NEN, 2011b), NEN 8702 for concrete structures (to be published) and so on. The load factors for the safety level 'repair', as used for bridge assessment in the Netherlands, are given in tables A1.2(B) and (C) of NEN 8700 (NEN, 2011a). These factors correspond to a reliability index $\beta_{rel} = 3{\cdot}6$ for consequence class 3 (Steenbergen and Vrouwenvelder, 2010). This class (NEN-EN 1990:2002 (CEN, 2002): table B1) defines a high consequence for the loss of human life or very great economic, social or environmental consequences. For dead loads, a factor $\gamma_{DL} = 1{\cdot}15$ is used and, for live loads, $\gamma_{LL} = 1{\cdot}3$.

For LRFRs according to the Aashto bridge evaluation manual (Aashto, 2011), the factors for design load at the operating level are used. Load ratings based on the operating rating level generally describe the maximum permissible live load to which the structure may be subjected and, as such, is described in a similar way as the repair level from NEN 8700

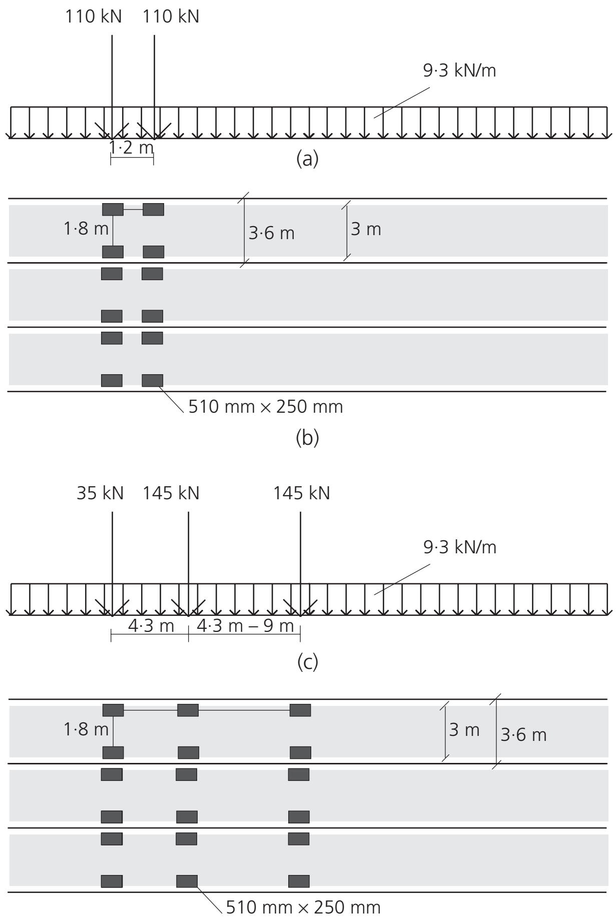

Figure 4. Loading as prescribed in Aashto (2015) with design tandem ((a) side view and (b) top view) and with design truck ((c) side view and (d) top view)

(NEN, 2011a). Allowing unlimited numbers of vehicles to use the bridge at operating level may shorten the life of the bridge. In table 6.A.4.2.2-1 of the bridge evaluation manual, the load factors are given as $\gamma_{DL} = 1{\cdot}25$ for the dead load, $\gamma_{DC} = 1{\cdot}50$ for superimposed loads and $\gamma_{LL} = 1{\cdot}35$ for live loads. The definition of the operating level is thus similar to the 'repair' level from NEN 8700. The target reliability index of these factors is $\beta_{rel} = 2{\cdot}5$ (Ghosn *et al.*, 2010) (which is considered as the lower bound for loss of human life in European practice) and is thus considerably lower than the index related to the Dutch 'repair' level.

4. Results from experimental research

4.1 Experiments on slabs failing in shear

Experimental research on a half-scale model of a solid-slab bridge was carried out at Delft University of Technology (Lantsoght *et al.*, 2013c, 2014, 2015a). Slabs of dimensions

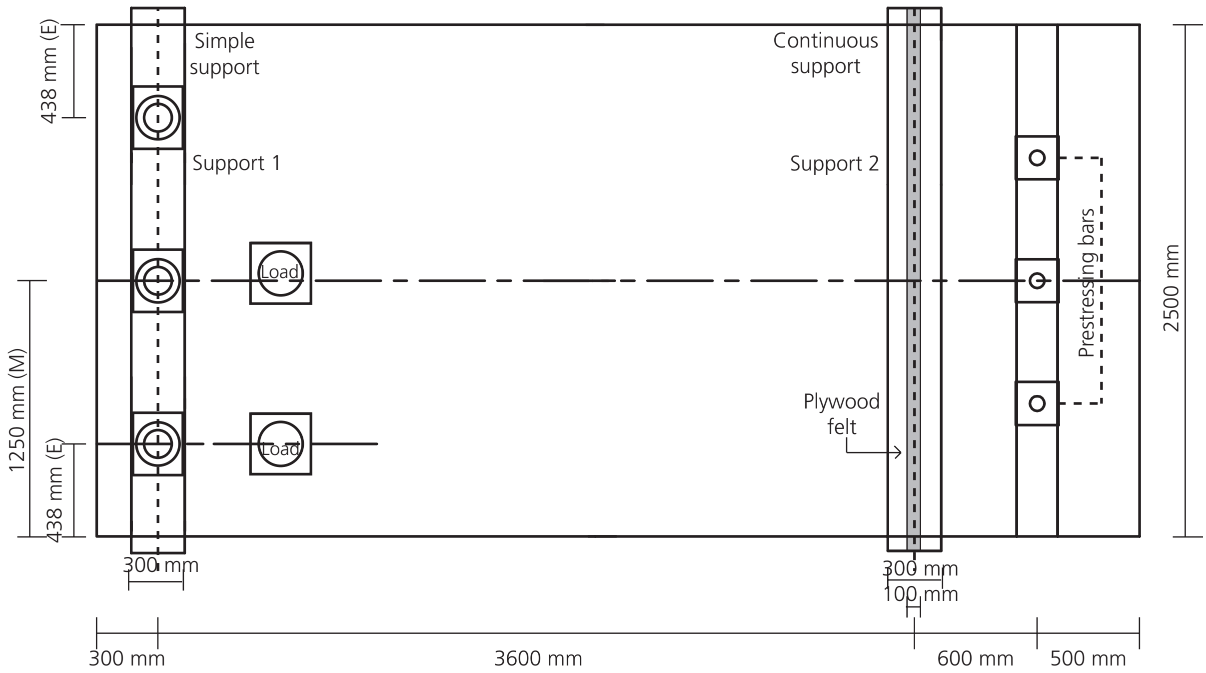

Figure 5. Top view of test setup for slabs under a concentrated load: supported by elastomeric bearings on the left and supported by a line support on the right. E indicates position of concentrated load close to the edge and M indicates position of concentrated load in the middle of the width

5 m × 2·5 m × 0·3 m and slab strips of 5 m × 0·3 m with variable widths were tested. A top view of the experimental setup is presented in Figure 5, showing two different support layouts. A displacement-controlled concentrated load was placed at different positions along the width and close to support 1 or close to support 2 at a variable distance to the support. In a second series of tests, a force-controlled constant line load of 240 kN/m at 1·2 m from the support was added. Different support conditions were also used – line support, three elastomeric bearings per side or a line of seven steel or elastomeric bearings. Support 1 is a simple support and support 2 is considered as a continuous support. Prestressing bars, anchored to the laboratory floor, were used to partially restrain the rotation at support 2 and thus create a moment over support 2.

In total, 26 slabs (18 under a concentrated load only and eight under a combination of loads) and 12 slab strips were tested. The properties of the specimens, the setup and loading were varied such that the following parameters could be studied: size of the loading plate; existing cracks and local failure; transverse flexural reinforcement; moment distribution at the support; distance between the concentrated load and the support; concrete compressive strength; overall width; reinforcement type (smooth bars or deformed bars), line support versus elastomeric bearings; and a combination of loads (Lantsoght *et al.*, 2012b, 2013b).

4.2 Choice of horizontal load spreading method and minimum effective width

Earlier research (Lantsoght *et al.*, 2015b) showed that the effective width as used in French practice is to be preferred. This conclusion was based on statistical analysis of the ratio of the tested to the predicted values (based on the shear formula from the Eurocode) and also on the results from the series of slab strips with increasing widths. The results of the experiments showed that the lower bound for the effective width (both for loading in the middle of the slab width and close to the edge) was equal to $4d_l$.

4.3 Increase in capacity close to support: β_{new}

To take into account the higher shear capacities of slabs, an additional enhancement factor reducing the contribution of concentrated loads to the total shear force was proposed (Lantsoght *et al.*, 2013a); this factor is equal to 1·25 (as a 5% lower bound of the ratio of the tested to predicted values for loads close to supports). The enhancement factor and the reduction factor $\beta = a_v/2d_l$ can be combined into $\beta_{new} = a_v/2{\cdot}5d_l$

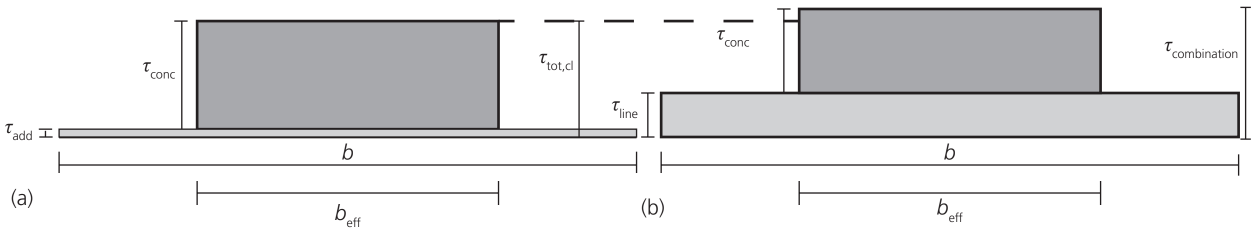

Figure 6. Superposition of shear stress due to a concentrated load over the effective width to the distributed load over the full slab width: (a) concentrated load only; (b) concentrated load and line load

for the case of concentrated loads on slabs with $0{\cdot}5d_l \leq a_v \leq 2{\cdot}5d_l$.

4.4 The hypothesis of superposition

In the literature and the resulting slab shear database, no reports are made of experiments on slabs under a combination of concentrated and distributed loads. In some experiments (Reißen and Hegger, 2013; Rombach and Latte, 2009), a small line load (edge load) was applied at the tip of a cantilevering deck, which is not representative of large distributed loads such as the dead load. The experiments carried out on slabs under a combination of loads prove that the hypothesis of superposition is valid; that is, the sum of the shear stress due to the concentrated load over the effective width (τ_{conc}) and the shear stress due to the distributed load at failure over the full width (τ_{line}) is larger than or equal to the ultimate shear stress in an experiment with a concentrated load only ($\tau_{tot,cl}$) (Figure 6).

4.5 The influence of flexure on the lower bound for shear

The expression for v_{min} (Equation 3) is based on the idea that, for low reinforcement ratios, the capacity can never be lower than the flexural capacity (Walraven, 2013) and assumes yielding of the longitudinal reinforcement at a characteristic yield strength $f_{yk} = 500$ MPa (Walraven, 2002) as well as sufficient anchorage capacity. However, most existing bridges are reinforced with lower grade steel. Before 1962, the standard reinforcement in the Netherlands was a type 'QR24' ($f_{yk} = 240$ MPa). Therefore, the expression for v_{min} is derived as a function of f_{yk} (Walraven, 2013). The resulting expression for v_{min} for lower grades of steel, assuming sufficient anchorage capacity, was found to be

9. $$v_{min} = 0{\cdot}772k^{3/2}f_{ck}^{1/2}f_{yk}^{-1/2}$$

For $f_{yk} = 500$ MPa, Equation 9 becomes Equation 3. The lower bound of the shear capacity is thus increased for elements reinforced with lower strength steel, as flexural failure will govern for a larger range of shear stresses. As a result, the unity check for flexure for cross-sections with a low flexural capacity will be higher and the governing failure mode will be flexure. Moreover, at the end supports, sufficient anchorage needs to be provided to apply Equation 9.

5. Practical applications: the quick scan approach

5.1 Eurocodes, the NEN 8700 series and recommendations

In 2008, a first quick scan method based on the Dutch codes was developed by Dutch structural engineering companies for the Ministry of Infrastructure and the Environment (Rijkswaterstaat). The Eurocodes, the NEN 8700 (NEN, 2011a) series and recommendations based on the experiments were implemented into the quick scan (QS-EC). Materials research on existing bridges indicated that, for the slab bridges owned by Rijkswaterstaat (designed and built in the same era), a minimum concrete cube compressive strength of 45 MPa can be assumed (Steenbergen and Vervuurt, 2012).

For superimposed loads, the thickness of the wearing surface is assumed to be 120 mm. Vertical stress redistribution through the asphalt layer is taken at a 45° angle, so that the Eurocode wheel print of 400 mm × 400 mm is replaced by a fictitious wheel print on the concrete surface of 640 mm × 640 mm.

All trucks are assumed to be centred in the fictitious lane. Based on the recommendations developed from the experimental research, the most unfavourable position (Figure 7) of the truck loads to determine the maximum shear force at the edge of the viaduct is obtained by placing the first design truck at $a_v = 2{\cdot}5d_l$. This distance is governing since the recommendations take the influence of direct load transfer into account up to $2{\cdot}5d_l$ (Rijkswaterstaat, 2013). For assessment of existing bridges, an asymmetric effective width is chosen in the first

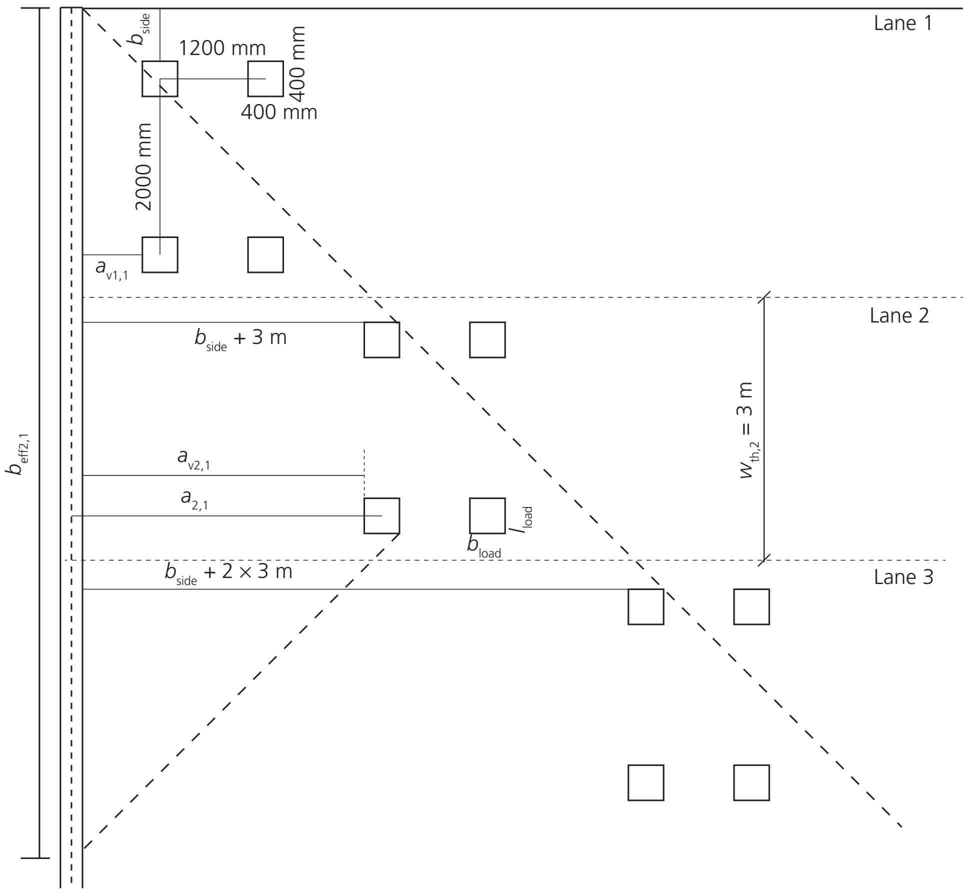

Figure 7. Most unfavourable position of design trucks

lane. Use of an asymmetric effective width results in the resultant force of the wheel load not coinciding with the resultant force of the distributed shear stress. In the second and third lanes, the design truck is placed so that the effective width (Figure 7) of the first axle starts at the edge of the viaduct.

The increased contribution of the lane load in the first lane to the resulting shear stress can be approximated based on a triangular distribution, as shown in Figure 8(a). The resulting shear force is then

10. $$V_{\text{addlane1}} = \frac{F}{b} + \frac{(Fe)y}{1/12b^3}$$

with

11. $$F = \left(\alpha_{q1} \times 9\,\text{kN/m}^2 - \alpha_{q2} \times 2{\cdot}5\,\text{kN/m}^2\right) w_{\text{th},1} \times \left(\frac{l_{\text{span}}}{2} - 2d_1 + \frac{1}{4}\frac{d_1}{2} + \frac{15}{16}d_1\right)$$

12. $$e = \left(\frac{1}{2}b - b_{\text{edge}} - \frac{w_{\text{th},1}}{2}\right)$$

13. $$y = \frac{1}{2}b - 2d_1$$

14. $$\Delta q_{\text{load}} = \alpha_{q1} \times 9\,\text{kN/m}^2 - \alpha_{q2} \times 2{\cdot}5\,\text{kN/m}^2$$

In the approach from Figure 8(a) it is assumed that the slab is infinitely stiff in the transverse direction but weak in torsion. A slab bridge, however, has torsional stiffness, which can be estimated with the approach of Guyon–Massonet. The proposed method from Figure 8(a) should give more conservative shear forces than the analysis based on the Guyon–Massonet method. To obtain this result, the maximum width b over which the triangular distribution is used is limited to $0{\cdot}72l_{\text{span}}$

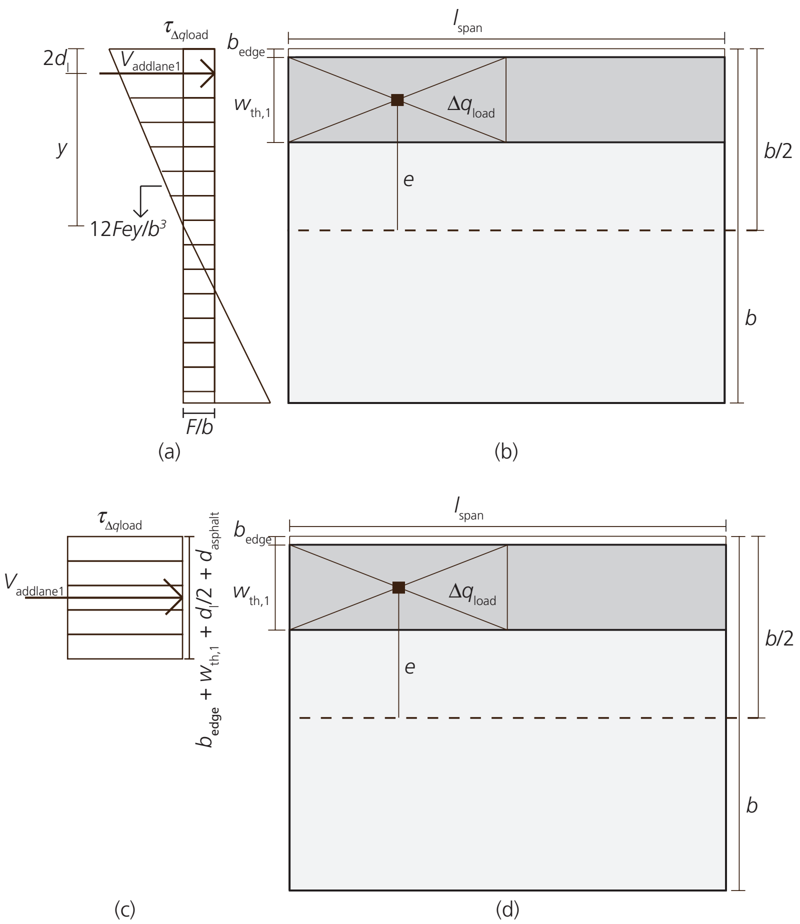

Figure 8. Model for contribution of increased loading in the first heavily loaded lane assuming a triangular stress distribution over the support: (a) assumed stress distribution $\tau_{\Delta q\text{load}}$ due to load and moment from eccentricity of load; (b) sketch of top view with location of first heavily loaded lane; (c) assumed stress distribution (note that the width is slightly larger than the lane width due to the vertical stress distribution to half the slab depth); (d) sketch of associated top view with location of first heavily loaded lane

(Lantsoght *et al.*, 2012a). A model factor of 1·1 is added. The lower bound of this approach is determined by a vertical load distribution under an angle of 45° to half the slab depth $d_l/2$, as shown in Figure 8(c)

$$F_{\min} = \left(\alpha_{q1} \times 9\,\text{kN/m}^2 - \alpha_{q2} \times 2{\cdot}5\,\text{kN/m}^2\right) \times \left[\min\left(b_{\text{edge}}, \frac{d_l}{2} + d_{\text{asphalt}}\right) + w_{\text{th},1} + \frac{d_l}{2} + d_{\text{asphalt}}\right] \tag{15}$$

The quick scan method was developed for statically determinate structures. As the shear force at the mid-support for statically indeterminate structures can be larger, the quick scan method needs to be altered for these cases. The solution is the use of correction factors, which were developed based on case studies of multiple-span structures (Lantsoght *et al.*, 2012a). The correction factor is the ratio of the shear force in the statically indeterminate case to the shear force in the statically determinate case. The cases that were studied are applicable within the scope of the quick scan: three or four spans, with end spans of $0{\cdot}7l_{\text{span}}$ and $0{\cdot}8l_{\text{span}}$, cross-sectional depths of 600–1000 mm and edge distances (distance between the free edge and the centre of the load, b_r) between 300 mm and 1400 mm.

5.2 Aashto LRFR and LRFD

A quick scan according to North American practice was also developed (QS-Aashto). Vertical force redistribution through $d_{\text{asphalt}} = 120$ mm is assumed at a 45° angle for the axle loads and to $d_l/2$ for the lane load. The spreadsheet selects whether the design tandem or design truck, assumed to be centred in the fictitious lane, results in the largest shear forces. The most unfavourable position of the vehicular loads to determine the maximum shear force at the edge of the

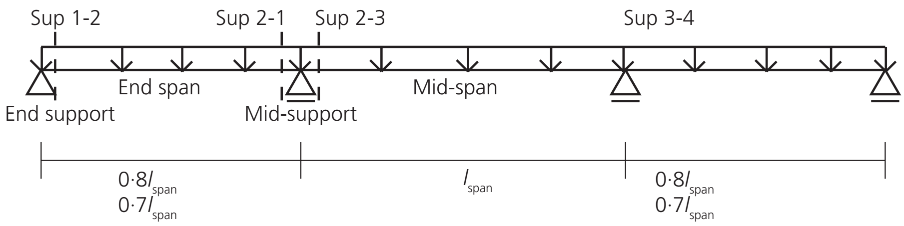

Figure 9. Considered sections for a typical three-span bridge

viaduct is obtained by placing the first wheel load at $a_v = d_l$. Additional factors for statical indeterminacy are developed for QS-Aashto. In accordance with §5.8.3.2 of Aashto LRFD (Aashto, 2015), the shear check is carried out at the face of the support. The cylinder compressive strength according to NEN-EN 1992-1-1:2005 (CEN, 2005) is transformed to f_c' by using (based on table 5.3.2.2 of ACI 318-11 (ACI, 2011))

$$f_c' = \frac{f_{ck} + 8\ \text{MPa} - 4{\cdot}28\ \text{MPa}}{1{\cdot}1} \tag{16}$$

5.3 Comparison based on ten selected cases

The calculation method based on the Eurocodes, the NEN 8700 (NEN, 2011a) series and experimental recommendations was compared to the calculations based on the bridge evaluation manual (Aashto, 2011) and LRFD (Aashto, 2015). Nine existing solid-slab bridges that are straight or have insignificant skew angles, with at least three spans and an (almost) constant cross-sectional depth were checked at a minimum of three different cross-sections (Figure 9) and at one section for the example reinforced concrete slab bridge (MBE-A7) from the Aashto bridge evaluation manual (Aashto, 2011). The results are shown in Table 1.

Comparing the results of the calculations shows that the occurring loading results in similar shear forces at the face of the support for both the Eurocode and Aashto approaches (average of $v_u/v_{Ed} = 1{\cdot}01$ with a standard deviation of 0·10). Two remarks are worthy of note

- the shear force due to the Aashto loading already incorporates the resistance factor $\phi = 0{\cdot}9$ while, in the QS-EC, a similar factor is incorporated on the capacity side of the equation
- the load factors from NEN 8700 (NEN, 2011a) result in higher reliability levels compared with the load factors from Aashto LRFR (Aashto, 2011).

The demands on the repair level from NEN 8700 (NEN, 2011a) and the 'design operating' level from Aashto LRFR (Aashto, 2011) are described similarly by the codes, but translated into a different reliability index. The limits of this comparison should be kept in mind.

Comparing the resulting shear capacities shows that QS-Aashto allows for higher shear capacities than QS-EC (average of $v_c/v_{Rd,c} = 2{\cdot}35$ with a standard deviation of 0·41). Both methods take the size effect into account, resulting in smaller shear capacities for larger depths. While the shear formula from NEN-EN 1992-1-1:2005 (CEN, 2005) results in shear capacities of < 0·50 MPa for low levels of flexural reinforcement ($\rho_l < 0{\cdot}6\%$), the influence on the calculated shear capacities according to QS-Aashto is smaller. The smallest shear capacity according to QS-Aashto of 0·754 MPa was obtained for a long span ($l/d_l = 19{\cdot}6$). The viaducts for which data from materials research are available ($f_{ck,cube} > 55$ MPa) result in higher shear capacities according to QS-Aashto compared with QS-EC, as Aashto uses a square root for the compressive strength and NEN-EN 1992-1-1:2005 (CEN, 2005) a cube root. The MCFT reduces the size of the aggregate (a_g) to 0 mm for high-strength concrete to account for the reduced aggregate interlock capacity in high-strength concrete (Vecchio and Collins, 1986). A similar limit is not found in Aashto LRFD (Aashto, 2015).

As a result, the unity checks according to the QS-Aashto are lower than those of the QS-EC. On average, the QS-Aashto unity check for shear is only 44% of the QS-EC unity check (with a standard deviation of 0·10). With the QS-EC, eight sections in five viaducts were identified as needing further investigation. With the QS-Aashto, all sections rated as sufficient. The MBE-A7 example does not require shear checking according to the bridge evaluation manual (Aashto, 2011), which is reflected by the small QS-Aashto unity check value. However, calculating this example with QS-EC results in a unity check value more than three times larger.

6. Summary and conclusions

Reinforced concrete slab bridges were used to study the differences and similarities between North American practice and the Eurocodes. A shear check was carried out at the support

							QS-EC			QS-Aashto		
Case	Section	b: m	d_l: m	l_{span}: m	$f_{ck,cube}$: MPa	ρ_l: %	v_{Ed}: MPa	$v_{Rd,c}$: MPa	Unity check	v_u: MPa	v_c: MPa	Unity check
1	sup 1-2	9·60	0·791	9·51	45·0	0·443	0·267	0·450	0·595	0·335	1·240	0·270
1	sup 2-1	9·60	0·791	9·51	45·0	0·517	0·401	0·473	0·847	0·452	1·110	0·407
1	sup 2-3	9·60	0·791	13·01	45·0	0·517	0·449	0·473	0·948	0·502	0·857	0·585
1	sup 3-4	9·60	0·791	15·53	45·0	0·583	0·517	0·493	1·048	0·580	0·754	0·769
2	sup 1-1	14·45	0·331	7·04	45·0	1·045	0·533	0·715	0·746	0·470	1·974	0·238
2	sup 2-1	14·45	0·331	7·04	45·0	1·045	0·715	0·715	0·999	0·618	1·624	0·381
2	sup 2-3	14·45	0·331	8·38	45·0	1·045	0·727	0·715	1·018	0·609	1·542	0·395
3	sup 1-1	11·92	0·600	7·08	58·3	0·429	0·280	0·534	0·524	0·310	1·680	0·184
3	sup 2-1	11·92	0·600	7·08	58·3	0·429	0·401	0·534	0·750	0·412	1·443	0·285
3	sup 2-3	11·92	0·600	8·38	58·3	0·429	0·403	0·534	0·755	0·398	1·369	0·290
4	sup 1-1	11·92	0·360	7·08	70·6	0·716	0·453	0·725	0·625	0·433	2·260	0·192
4	sup 2-1	11·92	0·360	7·08	70·6	0·716	0·618	0·725	0·853	0·570	1·809	0·315
4	sup 2-3	11·92	0·360	8·38	70·6	0·716	0·629	0·725	0·868	0·557	1·709	0·326
5	sup 1-2	13·60	0·542	9·50	48·4	0·817	0·444	0·615	0·723	0·454	1·616	0·281
5	sup 2-1	13·60	0·542	9·50	48·4	0·909	0·626	0·615	1·018	0·603	1·367	0·441
5	sup 2-3	13·60	0·542	12·50	48·4	0·909	0·640	0·615	1·041	0·640	1·183	0·541
6	sup 1-2	19·20	0·457	10·00	49·6	0·934	0·525	0·670	0·783	0·510	1·868	0·273
6	sup 2-1	19·20	0·457	10·00	49·6	0·934	0·722	0·670	1·077	0·684	1·509	0·453
6	sup 2-3	19·20	0·457	13·00	49·6	0·934	0·738	0·670	1·102	0·720	1·285	0·560
7	sup 1-2	14·75	0·540	9·50	37·3	0·770	0·437	0·553	0·789	0·444	1·512	0·294
7	sup 2-1	14·75	0·540	9·50	37·3	1·284	0·606	0·656	0·924	0·591	1·453	0·407
7	sup 2-3	14·75	0·540	14·00	37·3	1·284	0·680	0·656	1·037	0·699	1·195	0·585
8	sup 1-2	13·36	0·590	12·00	66·4	1·366	0·439	0·798	0·550	0·477	2·044	0·233
8	sup 2-1	13·36	0·590	12·00	66·4	1·573	0·639	0·837	0·763	0·656	1·755	0·374
8	sup 2-3	13·36	0·590	15·05	66·4	1·573	0·638	0·837	0·762	0·682	1·508	0·452
9	sup 1-2	12·50	0·650	10·00	74·6	0·55	0·372	0·773	0·481	0·407	1·940	0·210
9	sup 2-1	12·50	0·650	10·00	74·6	1·092	0·543	0·773	0·703	0·554	1·749	0·317
9	sup 2-3	12·50	0·650	15·00	74·6	1·092	0·609	0·773	0·788	0·657	1·426	0·461
MBE-A7		13·10	0·310	6·55	19·8	0·334	0·674	0·423	1·596	0·576	1·137	0·506

Table 1. Results of ten bridge case studies according to QS-EC and QS-Aashto

with a quick scan spreadsheet, resulting in a unity check, which is the ratio between the design shear stress and the design shear capacity.

Taking into account the load factors from the ‘repair’ level of NEN 8700 (NEN, 2011a) and the ‘design operating’ level of Aashto LRFR (Aashto, 2011) results in similar shear stresses at the support. Even though the descriptions of the requirements for the safety levels are similar in the codes, the underlying safety requirements, expressed as the required reliability index, are very different.

The resulting shear capacity according to QS-Aashto was found to be significantly higher than the shear capacity determined from QS-EC. A possible explanation for this is the lack of restriction on the concrete compressive strength in the Aashto LRFD specification (Aashto, 2015), while the underlying modified compression field theory reduces the size of the aggregates for high-strength concrete to take the lower aggregate interlock capacity into account.

The resulting unity checks according to QS-EC are higher than the unity checks according to QS-Aashto, indicating a more conservative approach to rate slab bridges in shear according to the Eurocodes. This outcome is not surprising because the safety demands underlying both procedures are different. These results do not indicate that all concrete slab bridges assessed according Aashto specifications can be considered satisfactory for shear, as the QS-EC was calibrated with experimental results and significantly higher unity checks are obtained with QS-EC than with QS-Aashto. Moreover, the code requirement from §6A.5.8 of Aashto LRFR (Aashto, 2011) – that in-service concrete bridges showing no visible signs of shear distress need not be checked for shear when rating – is not recommended when assessing an existing bridge. Finally, it should be noted that QS-EC combines the Eurocode provisions, the NEN 8700 provisions (NEN, 2011a) and recommendations from experimental results. As such QS-EC can be deemed more suitable for the assessment of existing slab bridges in shear.

Acknowledgement

The authors express their gratitude and sincere appreciation to the Dutch Ministry of Infrastructure and the Environment (Rijkswaterstaat) for financing this research work.

REFERENCES

Aashto (American Association of State Highway and Transportation Officials) (2011) *The Manual for Bridge Evaluation*. Aashto, Washington, DC, USA.

Aashto (2015) *AASHTO LRFD Bridge Design Specifications, 7th Edition with 2015 Interim Specifications*. Aashto, Washington, DC, USA.

ACI (American Concrete Institute) (2011) ACI Committee 318: Building code requirements for structural concrete (ACI 318-11) and commentary. ACI, Farmington Hills, MI, USA.

Aktan AE, Zwick M, Miller R and Shahrooz B (1992) Nondestructive and destructive testing of decommissioned reinforced concrete slab highway bridge and associated analytical studies. *Transportation Research Record* **1371**: 142–153.

Azizinamini A, Boothby TE, Shekar Y and Barnhill G (1994a) Old concrete slab bridges. 1. Experimental investigation. *Journal of Structural Engineering ASCE* **120(11)**: 3284–3304.

Azizinamini A, Shekar Y, Boothby TE and Barnhill G (1994b) Old concrete slab bridges. 2: Analysis. *Journal of Structural Engineering-ASCE* **120(11)**: 3305–3319.

CEN (Comité Européen de Normalisation) (2002) NEN-EN 1990:2002: Eurocode: Basis of structural design. Comité Européen de Normalisation, Brussels, Belgium, p. 103.

CEN (2003) NEN-EN 1991:2-2003: Eurocode 1: Actions on structures – part 2: traffic loads on bridges. CEN, Brussels, Belgium.

CEN (2005) NEN-EN 1992-1-1:2005: Eurocode 2: Design of concrete structures – part 1-1 general rules and rules for buildings. CEN, Brussels, Belgium.

Chauvel D, Thonier H, Coin A and Ile N (2007). Shear Resistance of slabs not provided with shear reinforcement, CEN/TC 250/SC 02 N 726, France, p. 32.

Cope RJ (1985) Flexural shear failure of reinforced-concrete slab bridges. *Proceedings of the Institution of Civil Engineers* **79(3)**: 559–583, http://dx.doi.org/10.1680/iicep.1985.838.

fib (International Federation for Structural Concrete) (2012) *Model Code 2010: Final Draft*. fib, Lausanne, Switzerland.

Ghosn M, Sivakumar B and Miao F (2010) Calibration of load and resistance factor rating methodology in New York State. *Transportation Research Record* **2200**: 81–89.

Lantsoght EOL, van der Veen C and Gijsbers FBJ (2012a) *Background Report to Spreadsheet for Checking at the Edge*. Delft University of Technology, Delft, the Netherlands, Stevin Report 25.5-12-14 (in Dutch).

Lantsoght EOL, van der Veen C and Walraven JC (2012b) Shear capacity of slabs and slab strips loaded close to the support. In *Recent Development in Reinforced Concrete Slab Analysis, Design and Serviceability*. ACI, Farmington Hills, MI, USA, ACI SP-287, 5.1–5.18.

Lantsoght EOL, van der Veen C, de Boer A and Walraven JC (2013a) Recommendations for the shear assessment of reinforced concrete slab bridges from experiments. *Structural Engineering International* **23(4)**: 418–426.

Lantsoght EOL, van der Veen C and Walraven JC (2013b) Shear capacity of slabs under a combination of loads. *Proceedings of fib Symposium on Engineering a Concrete Future: Technology, Modeling and Construction, Tel Aviv, Israel*, p. 12.

Lantsoght EOL, van der Veen C and Walraven JC (2013c) Shear in one-way slabs under a concentrated load close to the support. *ACI Structural Journal* **110(2)**: 275–284.

Lantsoght EOL, van der Veen C, de Boer A and Walraven JC (2014) Influence of width on shear capacity of reinforced concrete members. *ACI Structural Journal* **111(6)**: 1441–1450.

Lantsoght EOL, van der Veen C, de Boer A and Walraven JC (2015a) One-way slabs subjected to combination of loads failing in shear. *ACI Structural Journal* **112(4)**: 417–426.

Lantsoght EOL, de Boer A, van der Veen C and Walraven JC (2015b) Effective shear width of concrete slab bridges. *Institution of Civil Engineers – Bridge Engineering* **168(4)**: 287–298, http://dx.doi.org/10.1680/bren.13.00027.

Lantsoght EOL, van der Veen C, de Boer A and Walraven JC (2015c) Proposal for the extension of the Eurocode shear formula for one-way slabs under concentrated loads. *Engineering Structures* **95**: 16–24.

Lantsoght EOL, van der Veen C, Walraven JC and de Boer A (2015d) Database of wide concrete members failing in shear. *Magazine of Concrete Research* **67(1)**: 33–52, http://dx.doi.org/10.1680/macr.14.00137.

Lantsoght EOL, van der Veen C, Walraven JC and de Boer A (2015e) Transition from one-way to two-way shear in slabs under concentrated loads. *Magazine of Concrete Research* **67(17)**: 909–922, http://dx.doi.org/10.1680/macr.14.00124.

NEN (Dutch Normalisation Institute) (2011a) Normcommissie 351001: Assessment of structural safety of an existing structure at repair or unfit for use – basic requirements, NEN 8700:2011. NEN, Delft, the Netherlands (in Dutch).

NEN (2011b) Normcommissie 351001: Assessment of structural safety of an existing structure at repair or unfit for use – loads, NEN 8701:2011. NEN, Delft, the Netherlands (in Dutch).

Regan PE (1987) *Shear Resistance of Members without Shear Reinforcement; Proposal for CEB Model Code MC90*. Polytechnic of Central London, London, UK, pp. 1–28.

Reißen K and Hegger J (2013) Experimental investigations on the shear-bearing behaviour of bridge deck cantilever slabs under wheel loads. *Beton- und Stahlbetonbau* **108(5)**: 315–324 (in German).

Rijkswaterstaat (2013) *Guideline Assessment of Bridges – Assessment of Structural Safety of an Existing Bridge at Current Use, Repair and Unfit for Use*. Rijkswaterstaat, Utrecht, the Netherlands (in Dutch).

Rombach G and Latte S (2009) Shear resistance of bridge decks without transverse reinforcement. *Beton- und Stahlbetonbau* **104(10)**: 642–656 (in German).

Steenbergen RDJM and Vervuurt AHJM (2012) Determining the in situ concrete strength of existing structures for assessing their structural safety. *Structural Concrete* **13(1)**: 27–31.

Steenbergen RDJM and Vrouwenvelder ACWM (2010) Safety philosophy for existing structures and partial factors for traffic loads on bridges. *Heron* **55(2)**: 123–140.

Vecchio FJ and Collins MP (1986) The modified compression-field theory for reinforced-concrete elements subjected to shear. *Journal of the American Concrete Institute* **83(2)**: 219–231.

Vergoossen R, Naaktgeboren M, 't Hart M, de Boer A and Van Vugt E (2013) Quick scan on shear in existing slab type viaducts. *Proceedings of International IABSE Conference, Assessment, Upgrading and Refurbishment of Infrastructures, Rotterdam, the Netherlands*. IABSE, Rotterdam, the Netherlands, pp. 1–8.

Walraven JC (2002) *Background Document for EC-2, Chapter 6.2: Shear*. Delft University of Technology, Delft, the Netherlands.

Walraven JC (2010) Residual shear bearing capacity of existing bridges. In *Shear and Punching Shear in RC and FRC Elements*. fib, Lausanne, Switzerland, fib Bulletin 57, pp. 129–138.

Walraven JC (2013) *Minimum Shear Capacity of Reinforced Concrete Slabs without Shear Reinforcement: The Value* v_{min}. Delft University of Technology, Delft, the Netherlands, Stevin Report 25.5-12-04 (in Dutch).

WHAT DO YOU THINK?

To discuss this paper, please email up to 500 words to the editor at journals@ice.org.uk. Your contribution will be forwarded to the author(s) for a reply and, if considered appropriate by the editorial panel, will be published as discussion in a future issue of the journal.

Proceedings journals rely entirely on contributions sent in by civil engineering professionals, academics and students. Papers should be 2000–5000 words long (briefing papers should be 1000–2000 words long), with adequate illustrations and references. You can submit your paper online via www.icevirtuallibrary.com/content/journals, where you will also find detailed author guidelines.